
Efficient Long-Context LLM Inference via KV Cache Clustering

Jie Hu^{12*} Shengnan Wang^{2*} Yutong He¹ Ping Gong³ Jiawei Yi³
Juncheng Zhang³ Youhui Bai² Renhai Chen² Gong Zhang² Cheng Li³ Kun Yuan¹

¹Peking University ²Huawei Technologies ³University of Science and Technology of China

Abstract

Large language models (LLMs) with extended context windows have become increasingly prevalent for tackling complex tasks. However, the substantial Key-Value (KV) cache required for long-context LLMs poses significant deployment challenges. Existing approaches either discard potentially critical information needed for future generations or offer limited efficiency gains due to high computational overhead. In this paper, we introduce *Chelsea*, a simple yet effective framework for online KV cache clustering. Our approach is based on the observation that key states exhibit high similarity along the sequence dimension. To enable efficient clustering, we divide the sequence into chunks and propose *Chunked Soft Matching*, which employs an alternating partition strategy within each chunk and identifies clusters based on similarity. Chelsea then merges the KV cache within each cluster into a single centroid. Additionally, we provide a theoretical analysis of the computational complexity and the optimality of the intra-chunk partitioning strategy. Extensive experiments across various models and long-context benchmarks demonstrate that Chelsea achieves up to 80% reduction in KV cache memory usage while maintaining comparable model performance. Moreover, with minimal computational overhead, Chelsea accelerates the decoding stage of inference by up to $3.19\times$ and reduces end-to-end latency by up to $2.72\times$.

1 Introduction

With the increasing demand to tackle a diverse range of complex real-world applications, such as multi-round dialogues [1], Large Language Models (LLMs) have been capable of supporting context windows of up to 1M tokens [2–4]. However, deploying LLMs in long-context scenarios introduces substantial challenges, particularly related to the Key-Value (KV) cache. The KV cache stores the keys and values of all preceding tokens to avoid re-computation, and its memory requirements scale linearly with the context length. Due to the auto-regressive nature of LLMs, generating each token necessitates accessing the entire KV cache, making it a significant bottleneck for both inference latency and throughput. Moreover, the large size of KV cache imposes considerable demands on memory capacity, further complicating deployment.

To address these challenges, there is a pressing need for effective methods to reduce the KV cache size. Existing studies have explored this problem from multiple perspectives, including KV cache eviction [5–9], quantization [10, 11], and channel pruning [12], among others. By leveraging the inherent sparsity of the attention score matrix [5], various methods have been proposed to reduce redundancy along the sequence length dimension. However, these approaches exhibit notable limitations. KV cache eviction, which discards less critical tokens based on historical attention scores, often leads to

*Equal contribution.

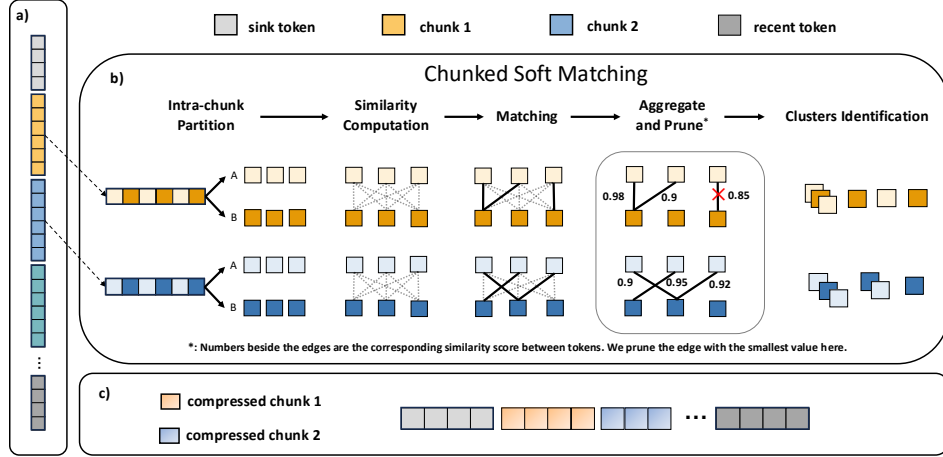


Figure 1: An overview of Chelsea: a) Divide sequences into chunks; b) Chunked Soft Matching to identify clusters; c) KV cache compression after clustering.

significant performance degradation. This occurs because tokens deemed unimportant in the current context may become crucial for future generations, especially in long-context scenarios. To mitigate this issue, KV cache merging techniques [13–15] have been introduced, aiming to merge tokens instead of evicting them. The primary difficulty in token merging lies in identifying suitable merging sets. Existing methods typically rely on preliminary token eviction or traditional nearest neighbor matching, both of which limit their ability to maintain model performance. Moreover, the merging process itself introduces substantial computational overhead, posing further challenges to achieving practical acceleration in large language model inference.

Our approach is inspired by a key observation: key states exhibit high similarity along the sequence dimension, as illustrated in Fig. 2. This insight motivates us to cluster the KV cache by identifying merging sets solely based on token similarity. However, efficiently and accurately performing KV cache clustering online remains challenging, particularly given the long sequence lengths involved.

In this paper, we introduce Chelsea, a simple yet effective online KV cache clustering framework that improves the inference efficiency of LLMs in long-context scenarios. The core innovation of Chelsea is the *Chunked Soft Matching* algorithm, which enables efficient KV cache clustering without compromising model performance. Inspired by the Bipartite Soft Matching algorithm [16] for Vision Transformers [17], we are the first to extend this idea to the context of KV cache compression. The framework begins by dividing the sequence into chunks. Based on the observed correlation between token similarity and positional distance, we further partition each chunk in an alternating manner and theoretically prove the optimality of this intra-chunk partitioning strategy. Subsequently, *Chunked Soft Matching* identifies clusters by locating highly similar token pairs across all chunks. Finally, the corresponding keys and values within each cluster are merged into a single centroid.

We conduct extensive experiments to evaluate both the effectiveness and efficiency of Chelsea. The results demonstrate that Chelsea can reduce the KV cache memory usage by up to 80% while maintaining comparable model performance. Furthermore, by dynamically clustering to preserve contextual information, Chelsea outperforms baselines under a limited cache budget. Additionally, due to its simplicity and efficiency, Chelsea accelerates the decoding stage of LLM inference by up to $3.19\times$ and reduces end-to-end latency by up to $2.72\times$.

Our contributions are summarized as follows.

- We introduce Chelsea, a simple yet effective framework for online KV cache clustering. The core innovation of Chelsea is a novel clustering algorithm, termed *Chunked Soft Matching*.
- Chelsea is a lightweight, plug-and-play solution to improve LLM inference efficiency. We theoretically analyze its computational complexity and formally prove the optimality of the intra-chunk partitioning strategy based on the observed similarity patterns.

- Chelsea achieves up to an 80% reduction in KV cache memory usage with minimal impact on model performance. Additionally, it accelerates the decoding stage by up to $3.19\times$ and reduces end-to-end latency by up to $2.72\times$.

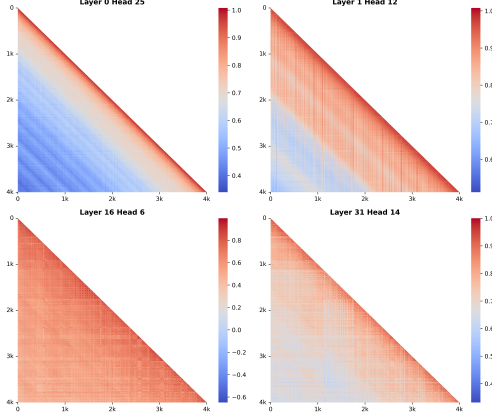


Figure 2: The cosine similarity maps of key states across various layers and heads.

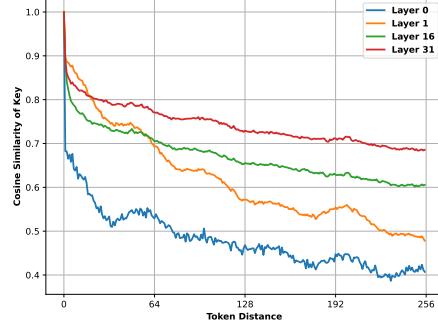


Figure 3: The correlation between token distance and the cosine similarity of key states.

2 Related Work

KV Cache Eviction. Eviction-based methods focus on selectively maintaining a fixed-size KV cache during the decoding stage. H2O [5] retains a limited budget of KV cache by greedily discarding unimportant tokens based on the accumulated attention score. StreamingLLM [6] preserves the initial few tokens along with the recent tokens, based on the identification of attention sinks. SnapKV [8] selects important tokens for each attention head based on the observation window of prompts. FastGen [7] conducts profiling for attention heads and dynamically evicts tokens based on different attention patterns. However, these methods suffer from performance degradation in the long context scenario, since the information of the discarded token will be lost permanently.

KV cache merging. CaM [13] adaptively merges to-be-evicted value states into the remaining value cache. D2O [15] introduces a compensation mechanism that merges discarded tokens with similar ones. Both methods rely heavily on preliminary token eviction, which limits their ability to preserve model performance. Squeezed Attention [18] and ClusterKV [19] employ offline K-means clustering to faster retrieve important tokens. However, K-means clustering incurs substantial computational overhead, making it impractical for online scenarios. KVMerger [14] proposes an effective KV cache merging algorithm based on token similarity. However, its merging sets are constrained to be sequentially consecutive, and the similarity computations remain computationally expensive.

Bipartite Soft Matching. Introduced by ToMe [16], Bipartite Soft Matching (BSM) is an algorithm designed to merge tokens in Vision Transformers (ViT) [17], which is as fast as token pruning. Recent studies [20–22] have extended BSM to enhance the efficiency of ViTs and Stable Diffusion [23] without compromising model performance.

3 Preliminary

In this section, we first give a basic preliminary about the KV cache clustering in LLM inference. For simplicity, we focus on a single attention head within a specific layer. LLM inference consists of two stages: pre-filling and decoding. During the pre-filling stage, the model generates the first token and initializes the KV cache, which stores the key and value states of the prompt as $K \in \mathbb{R}^{n \times d}$ and $V \in \mathbb{R}^{n \times d}$, respectively. In the decoding stage, for the given states of the current input $q, k, v \in \mathbb{R}^{1 \times d}$, KV cache is updated as $K = [K, k]$, $V = [V, v]$. The vanilla attention output is then computed as

follows:

$$\text{Attn}(q, K, V) = \text{softmax} \left(\frac{qK^T}{\sqrt{d_k}} \right) V = \frac{\sum_{i=1}^n \exp \left(\frac{q^T k_i}{\sqrt{d_k}} \right) v_i}{\sum_{i=1}^n \exp \left(\frac{q^T k_i}{\sqrt{d_k}} \right)}. \quad (1)$$

For clearer derivation, we decompose KV cache into individual tokens, represented as $K = [k_1, \dots, k_n]$ and $V = [v_1, \dots, v_n]$, where each $k_i \in \mathbb{R}^d$ and $v_i \in \mathbb{R}^d$. In our approach, we utilize the cosine similarity as the distance metric between key states:

$$\cos(k_i, k_j) = \frac{k_i \cdot k_j}{\|k_i\| \|k_j\|}$$

Assume that tokens are grouped into clusters based on the similarity of their key states. The cluster centers are denoted as $\hat{K} = [\hat{k}_1, \dots, \hat{k}_C]$, where C represents the number of clusters. The number of tokens in each cluster is denoted by $N = [n_1, \dots, n_C]$, with each cluster center \hat{k}_t associated with a set of tokens $[\hat{k}_{1,t}, \dots, \hat{k}_{n_t,t}]$, corresponding to the tokens in the t -th cluster. Here, n_t is referred to as the cluster degree.

By approximating the attention output using the cluster centers in place of the original key states, the resulting attention output is as follows:

$$\begin{aligned} \text{Attn}(q, K, V) &= \frac{\sum_{t=1}^C \sum_{i=1}^{n_t} \exp \left(\frac{q^T k_{i,t}}{\sqrt{d_k}} \right) v_{i,t}}{\sum_{t=1}^C \sum_{i=1}^{n_t} \exp \left(\frac{q^T k_{i,t}}{\sqrt{d_k}} \right)} \\ &\approx \frac{\sum_{t=1}^C \sum_{i=1}^{n_t} \exp \left(\frac{q^T \hat{k}_t}{\sqrt{d_k}} \right) v_{i,t}}{\sum_{t=1}^C \sum_{i=1}^{n_t} \exp \left(\frac{q^T \hat{k}_t}{\sqrt{d_k}} \right)} \\ &= \frac{\sum_{t=1}^C \left[\exp \left(\frac{q^T \hat{k}_t}{\sqrt{d_k}} \right) \sum_{i=1}^{n_t} v_{i,t} \right]}{\sum_{t=1}^C n_t \exp \left(\frac{q^T \hat{k}_t}{\sqrt{d_k}} \right)}. \end{aligned}$$

By merging the value states corresponding to the same indices as the key states, namely $\hat{v}_t = \frac{\sum_{i=1}^{n_t} v_{i,t}}{n_t}$, we formulate the approximate attention output, denoted as AppAttn, as follows:

$$\begin{aligned} \text{Attn}(q, K, V) &\approx \frac{\sum_{t=1}^C n_t \exp \left(\frac{q^T \hat{k}_t}{\sqrt{d_k}} \right) \hat{v}_t}{\sum_{t=1}^C n_t \exp \left(\frac{q^T \hat{k}_t}{\sqrt{d_k}} \right)} \\ &= \frac{\sum_{t=1}^C \exp \left(\frac{q^T \hat{k}_t}{\sqrt{d_k}} + \log n_t \right) \hat{v}_t}{\sum_{t=1}^C \exp \left(\frac{q^T \hat{k}_t}{\sqrt{d_k}} + \log n_t \right)} \\ &\triangleq \text{AppAttn}(q, \hat{K}, \hat{V}, N), \end{aligned} \quad (2)$$

where $\hat{V} = [\hat{v}_1, \dots, \hat{v}_C]$. (2) demonstrates that the approximate attention after clustering aligns with the vanilla attention in (1) when each token is treated as a separate cluster. To minimize output error, it is essential that the key states within each cluster exhibit high similarity. Fortunately, the following observations further support the viability of this approach.

4 Observations

In this section, we present several empirical observations that motivate our approach.

Observation 1. Key states exhibit high, localized similarity along the sequence dimension.

Using the Llama-2-7B-32K model [24], we randomly sample sequences of length 4K from the WikiText-2 [25] dataset and perform zero-shot inference. The cosine similarity maps of the key states

are visualized in Fig. 2. We observe that key states exhibit high cosine similarity between tokens across different layers and heads. Notably, tokens with high similarity tend to cluster within localized regions. These findings align with previous work [14].

This observation suggests that KV cache clustering can be leveraged for efficient inference without compromising accuracy. Furthermore, the observed localized similarity motivates us to subsequently enhance clustering efficiency by identifying similar tokens within local regions, rather than considering the entire sequence.

Observation 2. As token distance increases, the cosine similarity of key states generally decreases monotonically and follows a convex trend.

Building on the observed localized similarity, we further investigate the correlation between token distance and the cosine similarity of key states. We randomly sample multiple tokens within the sequence, define the local region as 256 tokens, and compute the average similarity across samples and attention heads. As illustrated in Fig. 3, we find that as token distance increases, the cosine similarity between key states generally follows a monotonically decreasing trend. Furthermore, this correlation appears to be convex with respect to the distance.

This observation motivates our framework design of a highly efficient clustering algorithm that minimizes the computational complexity of identifying similar token sets. Additionally, it provides empirical support for the theoretical analysis in Sec. 6 which proves the optimality of the partitioning strategy in our framework.

Observation 3. Not all layers and heads are equal in KV cache clustering.

Recent studies have explored the varying behaviors of different layers and attention heads in LLMs [26–31]. These findings indicate that applying a uniform clustering ratio across all layers and heads does not lead to optimal performance.

As shown in Fig. 3, the initial layers exhibit lower similarity compared to subsequent layers. Attention heads that are more sensitive to similarity-based clustering are referred to as outlier heads. Detailed visualizations of these outlier heads can be found in Appendix B.

5 Method

In this section, we introduce Chelsea, a simple yet effective framework for KV cache clustering designed to enhance the efficiency of long-context LLM inference. The framework comprises three key steps. First, the sequence is divided into chunks while preserving the attention sinks and recent tokens. Second, we propose a novel KV cache clustering algorithm, termed *Chunked Soft Matching*, which employs an alternating partition strategy within each chunk and identifies clustering sets by finding highly similar token pairs across all chunks. Finally, the key and value states are merged based on the identified clusters, yielding a compressed KV cache for subsequent generations. An overview of Chelsea is depicted in Fig. 1.

5.1 Overall Inference Pipeline

In our framework, the cache budget is predefined as $B = R \cdot (n + \Gamma)$, where R denotes the cache ratio and $n + \Gamma$ represents the sum of the prompt length and the maximum decoding length. When the cache length s exceeds the threshold $B + g$, Chelsea is invoked to compress the cache length to B . Hence, clustering is performed every g step during the decoding stage. The overall pipeline of LLM inference integrated with Chelsea is illustrated in Algorithm 1, with the process of Chelsea depicted in Fig. 1.

Chelsea primarily employs the Chunked Soft Matching algorithm to compress the KV cache. r represents the compression ratio that governs the proportion of pruned edges in Fig. 1. Given that Bipartite Soft Matching mechanism can only reduce the cache size by at most half at each step, multiple clustering steps are required to ensure the KV cache is compressed within the budget.

Algorithm 1 Inference Pipeline with Chelsea

Require: cache ratio R , compression ratio r , maximum decoding length Γ , attention sink n_1 , recent budget n_2 , interval step g , chunk size c .
Pre-filling: $Q, K, V \in \mathbb{R}^{n \times d}$. Initialize: Cache length $s = n$, Cluster degree $N = [1] \cdot n$, Cache budget $B = R \cdot (n + \Gamma)$. Output: $O = \text{FlashAttn}(Q, K, V)$.
if $s \geq B + g$ **then**
 $K, V, N, s = \text{Chelsea}(K, V, N, s, n_1, n_2, r, c)$
end if
for $i = 1 \dots \Gamma - 1$ **do**
 Decoding states $q, k, v \in \mathbb{R}^{1 \times d}$. Update: $K = [K, k]$, $V = [V, v]$, $N = [N, 1]$, $s = s + 1$.
 Output: $O = \text{Softmax}(\frac{qK^T}{\sqrt{d}} + \log N)V$
 if $s \geq B + g$ **then**
 $K, V, N, s = \text{Chelsea}(K, V, N, s, n_1, n_2, r, c)$
 end if
end for

Table 1: Computational complexity of distance matrix. n is the sequence length and d is hidden dimension. k and i of K-Means refer to number of cluster centers and iterations. c of Chunked Soft Matching (CSM) refers to chunk size, which is relatively small to n .

Mesh	K-Means	BSM	CSM
n^2d	$inkd$	$\frac{1}{4}n^2d$	$\frac{1}{4}ncd$

5.2 Chunked Soft Matching

Based on Observation 1 in Sec. 4, Chelsea begins by dividing the key states into chunks, as illustrated in Fig. 1. The localized similarity of key states ensures that this approach will not cause a significant loss of accuracy. We keep the attention sink and recent tokens before partitioning, regarding their importance for model performance [5, 6].

Inspired by the Bipartite Soft Matching (BSM) algorithm introduced by [16] for token merging in the transformer block of Vision Transformers (ViT) [17], we propose Chunked Soft Matching (CSM) for KV cache clustering in the second step of Chelsea.

BSM begins by partitioning the input tokens into two distinct sets, A and B . Next, for each token in set A , an edge is drawn to its most similar token in set B . Among these edges, only the top-ranked similar connections are retained. Tokens that remain connected through these edges are then merged into a cluster, while others are left unchanged. Finally, the two sets, A and B , are concatenated to form the output, incorporating both merged and unchanged tokens.

However, directly applying BSM for KV cache clustering poses two significant challenges. The first challenge arises from the large sequence dimension in long-context scenarios, which leads to inefficiencies in the matching process. The second challenge involves optimally partitioning the sequence into two sets, A and B , in a way that minimizes the impact on model accuracy.

CSM addresses the first challenge by its previous chunking step, directly improving efficiency. While there are various potential approaches for KV cache clustering, such as K-means, these typically require multiple iterations to define clusters, resulting in substantial computational overhead. We compare the computational complexity of different methods in Table 1. The "Mesh" method involves computing the cosine similarity between all token pairs.

Building on Observation 2 in Sec. 4, we address the second challenge by partitioning each chunk into two sets, A and B , in an alternating manner. The core idea of CSM is to assign highly similar states to different sets, ensuring that token pairs with high similarity are placed between sets, rather than within them. Furthermore, based on the observed monotonically decreasing and convex trend, we rigorously demonstrate the theoretical optimality of this intra-chunk partitioning strategy in Sec. 6. After computing the similarities, CSM aggregates the edges from all chunks and prunes those with

relatively low similarity scores. Finally, the clustering sets are identified as collections of tokens connected by the remaining edges.

5.3 KV Cache Compression

After identifying the clusters, KV cache should be merged according to a specific rule. As illustrated in Algorithm 1, clustering occurs multiple times, thereby it is essential to track the degrees n_t of each token. In our approach, key and value states are merged within each cluster, weighted by the degree of the tokens. For a cluster set k_1, k_2, \dots, k_t , each associated with degrees n_1, n_2, \dots, n_t , the merged key states is computed as:

$$\hat{k} = \frac{n_1 k_1 + n_2 k_2 + \dots + n_t k_t}{n_1 + n_2 + \dots + n_t}$$

The value states are merged in the same manner, weighted by their respective degrees. Once the key and value states are compressed, they are concatenated with the preserved attention sink and recent states to form the new compressed sequence for the next decoding step.

5.4 Offline Calibration for Outlier Head

Based on Observation 3 in Sec. 4, we find that certain outlier heads require the full KV cache during generation. Specifically, the positions of these outlier heads remain consistent across datasets. Therefore, we identify the outlier heads through offline calibration. We conduct the inference process on the widely used calibration dataset WikiText-2 [25]. Detailed information regarding the outlier heads is provided in Appendix B.

6 Theoretical Results

In this section, we theoretically justify the optimality of our partitioning strategy which divides each chunk into two sets A and B in an alternating manner.

Intuitively, the partitioning strategy should retain the edges with the highest similarities to yield better clusters. Based on Observation 2 in Sec. 4, we consider a convex and monotonically decreasing score function $f : \mathbb{N} \rightarrow \mathbb{R}$ that maps the distance to an importance score. With the score function f , the optimal partitioning can be achieved by solving the following optimization problem:

$$\max_{A, B} \sum_{x \in A} \sum_{y \in B} f(|x - y|). \quad (3)$$

The following theorem states that, for any score function f that is convex and monotonically decreasing, the alternating partitioning strategy we propose is always the optimal solution of problem (3).

Theorem 6.1. *Define partition set $\mathcal{P}_{2n} = \{(A, B) \mid |A| = |B| = n, \text{ and } A \cup B = [2n]\}$. If function $f : [2n - 1] \rightarrow \mathbb{R}$ satisfies $f(1) - f(2) \geq f(2) - f(3) \geq \dots \geq f(2n - 2) - f(2n - 1) \geq 0$, it holds that*

$$(A_0, B_0) = (\{1, 3, \dots, 2n - 1\}, \{2, 4, \dots, 2n\}) \\ \in \arg \max_{(A, B) \in \mathcal{P}_{2n}} \sum_{x \in A} \sum_{y \in B} f(|x - y|).$$

Here, we use notation $[k]$ to denote the set of positive integers no larger than k , i.e., $[k] := [1, k] \cap \mathbb{Z}$.

7 Experiments

In this section, we conduct comprehensive experiments to evaluate the effectiveness and efficiency of Chelsea, followed by the ablation study on the framework design.

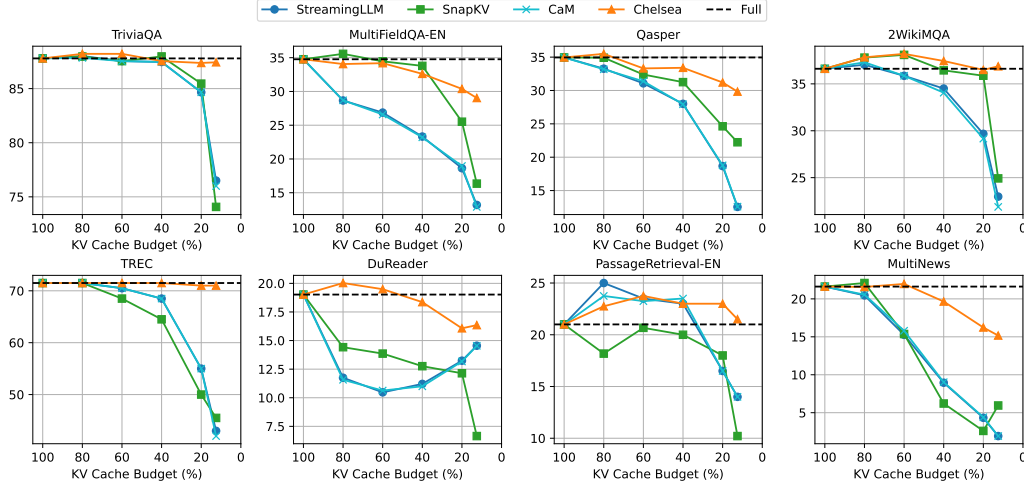


Figure 4: Performance comparison on Llama-2-7B-32K using LongBench datasets.

Table 2: Performance comparison of Chelsea and other KV cache compression baselines under 20% cache budget across various LLMs on LongBench.

	Method	NrrQA	Qasper	MF-en	HotpotQA	2WikiMQA	Musique	DuReader	MultiNews	TREC	TriviaQA	SAMSum	PCount	Pre	Lcc	Avg
Llama-2-7B	Full	20.53	34.95	34.77	49.11	36.61	21.87	19.02	21.62	71.5	87.79	43.89	1.5	21.0	50.84	36.79
	StreamingLLM	16.72	18.67	18.63	41.6	29.67	16.69	13.24	4.33	55.0	84.66	37.95	2.0	16.5	29.98	27.55
	SnapKV	21.78	24.63	25.52	45.72	35.87	20.45	12.14	2.6	50.0	85.46	40.04	2.0	18.0	25.58	29.27
	CaM	18.04	18.78	18.96	41.25	29.16	16.91	13.17	4.4	55.0	84.66	38.78	2.0	16.5	29.84	27.68
	Chelsea	22.74	31.2	30.38	46.51	36.49	20.49	16.07	16.23	71.0	87.37	40.86	2.0	23.0	47.37	35.12
Llama-3.1-8B	Full	31.69	26.25	28.71	17.01	16.3	11.59	29.67	26.91	72.5	91.65	43.94	5.35	98.23	52.16	39.43
	StreamingLLM	26.62	13.49	16.74	12.36	13.14	7.88	14.03	22.31	65.0	89.74	42.36	7.01	93.58	50.41	33.90
	SnapKV	31.51	18.21	22.45	15.42	14.64	11.88	19.55	23.02	64.0	90.53	42.27	6.5	97.46	51.84	36.38
	CaM	27.05	13.76	16.31	12.62	12.88	7.78	14.06	22.29	65.0	89.79	41.83	7.61	93.54	50.24	33.91
	Chelsea	31.61	20.37	26.32	16.52	15.61	11.42	24.08	24.33	73.5	91.25	41.45	6.28	97.98	49.52	37.87
Qwen2-7B	Full	25.42	45.92	48.22	42.89	44.99	24.8	26.38	26.13	52.50	84.09	35.64	5.5	70.50	47.16	41.44
	StreamingLLM	22.82	31.67	27.46	34.25	37.23	17.69	16.35	20.74	45.00	83.43	34.05	5.0	29.5	44.17	32.10
	SnapKV	25.92	37.91	44.23	41.15	43.97	24.32	21.34	21.98	40.00	83.74	34.59	5.5	65.5	44.77	38.21
	CaM	22.63	31.91	27.17	34.33	37.69	17.65	16.34	21.05	45.00	83.5	33.91	5.0	28.5	43.84	32.04
	Chelsea	24.8	43.6	44.27	41.39	42.81	24.84	22.2	22.57	51.0	84.56	33.39	5.0	71.5	47.25	39.94

7.1 Experimental Settings

Tasks and Models. We evaluate Chelsea using the widely recognized benchmarks, LongBench [32] and Needle-in-a-Haystack (NIAH) [33], which are designed to assess the long-context understanding capabilities of LLMs. LongBench includes 21 datasets covering six application scenarios: single-document QA, multi-document QA, summarization, few-shot learning, synthetic tasks, and code completion. For evaluation, we employ three long-context models: Llama-2-7B-32K [24], Llama-3.1-8B-Instruct [34], and Qwen2-7B-Instruct [35], serving as the backbone LLMs.

Baselines. We compare Chelsea against state-of-the-art KV cache compression methods, typically representative cache eviction and merging methods, including StreamingLLM [6], SnapKV [8] and CaM [13]. Since the original design of H2O [5] is incompatible with FlashAttention, it cannot support long contexts due to memory constraints. Therefore, to enable H2O for long-context inference, we apply FlashAttention during the pre-filling stage and collect attention scores from the last several tokens, following [36]. Notably, replacing the historical attention score with recent tokens during the pre-filling stage resembles SnapKV [8].

Implementation Details. We implement all methods in the HuggingFace transformers codebase [37]. We set 16 attention sinks and 64 recent tokens for Chelsea. The default chunk size is 256 and the ratio of outlier heads is 4%. The default number format is BFloat16. Further experimental details are provided in Appendix C. All experiments are conducted using high-performance GPUs, featuring over 100 TFLOPS of processing power.

Table 3: Decoding latency and GPU memory usage (GB) comparison across varying context lengths on Llama-3.1-8B-Instruct. TTFT(s) and TPOT(s) are based on HuggingFace Transformers.

Context Length	16k			32k			64k		
	TTFT	TPOT	Memory	TTFT	TPOT	Memory	TTFT	TPOT	Memory
Full	1.784	0.043	19.38	4.212	0.071	23.53	11.421	0.137	31.83
CaM	1.781	0.068	25.55	4.201	0.106	35.50	11.435	0.180	55.40
Chelsea	1.814	0.035 (1.23\times)	15.86	4.306	0.036 (1.97\times)	16.69	11.500	0.043 (3.19\times)	18.36

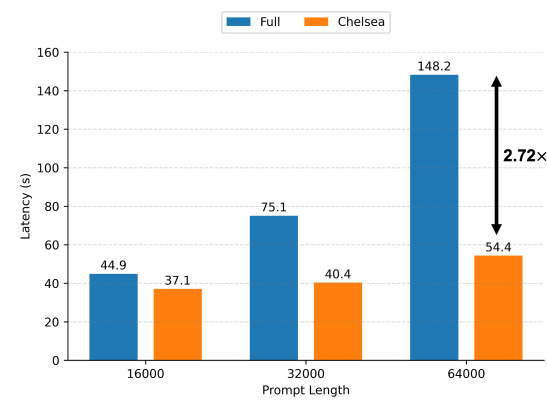


Figure 5: End-to-end latency with a decoding length of 1000 tokens on Llama-3.1-8B-Instruct.

Table 4: Performance of Chelsea with different chunk size under 20% cache budget. Chunk size has a relatively small effect on accuracy within a certain range.

Chunk Size	16	64	256	w/o chunk
Avg. Score	41.83	42.68	42.54	42.81

Table 5: Comparison of Chelsea with and without outlier heads. Outlier heads identification is crucial for model performance.

Method	w/o Outlier Head	Chelsea
Avg. Score	36.46	38.97

7.2 Accuracy Evaluation

We evaluate all methods on the LongBench benchmark, varying the KV cache budget from 12.5% to 80%. Table 2 presents a comparison of different methods across various LLMs under a fixed 20% KV cache budget, and Fig. 4 shows the performance trends of these methods on Llama-2 across different budgets. Additional results of LongBench and Needle-in-a-Haystack are provided in Appendix D.1.

The results consistently demonstrate that Chelsea outperforms existing methods across various tasks and models. Notably, Chelsea achieves up to 80% cache memory savings while maintaining comparable performance to full attention on most tasks.

7.3 Efficiency Evaluation

For efficiency, we evaluate both the decoding latency and the memory usage of models under 20% cache budget. Specifically, we measure two key metrics for LLM inference: Time To First Token (TTFT) and Time Per Output Token (TPOT). As shown in Table 3, Chelsea significantly accelerates the decoding stage with minimal overhead to the pre-filling stage, whereas existing merging techniques fail to deliver actual speedup. In addition, Chelsea reduces memory footprint compared to full attention. As sequence length increases, our framework achieves up to 3.19 \times faster decoding. As illustrated in Fig. 5, Chelsea outperforms full attention in terms of end-to-end latency, reducing the latency by up to 2.72 \times . Additional results are presented in Appendix D.2.

7.4 Ablation Study

Importance of chunking. In addition to the theoretical analysis in Table 1, we empirically demonstrate the necessity of chunking in Chelsea to minimize the extra overhead and achieve remarkable acceleration. Detailed latency analysis is provided in Table 10 of Appendix D.3.

Chunk size. To assess the impact of chunk size on accuracy, we select subsets of LongBench and conduct experiments across different chunk sizes, illustrated in Table 4. The results indicate that chunk size has a relatively small effect on the model performance within a certain range.

Importance of outlier heads. To evaluate the importance of outlier heads for model performance, we conduct evaluation on LongBench and the average score is shown in Table 5. Detailed accuracy and further analysis are presented in the Appendix D.3.

8 Conclusion and Limitations

This paper presents Chelsea, a simple yet effective framework for online KV cache clustering that improves the efficiency of long-context LLM inference. Chelsea reduces KV cache memory usage by up to 80% without compromising accuracy on most tasks, while accelerating the decoding stage by up to $3.19\times$ and reducing end-to-end latency by up to $2.72\times$. However, our work focuses on compressing the KV cache on the GPU and does not investigate memory offloading strategies. A promising direction for future research is to perform clustering on the CPU and transfer the resulting centroids to the GPU. Additionally, Chelsea currently employs a manually specified, static compression ratio and restricts cache reduction to at most half at each clustering step. This could be addressed by designing a dynamic compression strategy in future work.

References

- [1] R. Thoppilan, F. Xu, C. Chen, Y. Luan, S. Zhang, and I. Sutskever, “Chatgpt: Optimizing language models for dialogue,” *OpenAI Blog*, 2022. [Online]. Available: <https://openai.com/research/chatgpt-optimizing-language-models-for-dialogue>
- [2] J. Achiam, S. Adler, S. Agarwal, L. Ahmad, I. Akkaya, F. L. Aleman, D. Almeida, J. Altenschmidt, S. Altman, S. Anadkat *et al.*, “Gpt-4 technical report,” *arXiv preprint arXiv:2303.08774*, 2023.
- [3] H. Touvron, T. Lavril, G. Izacard, X. Martinet, M.-A. Lachaux, T. Lacroix, B. Rozière, N. Goyal, E. Hambro, F. Azhar *et al.*, “Llama: Open and efficient foundation language models,” *arXiv preprint arXiv:2302.13971*, 2023.
- [4] G. Team, P. Georgiev, V. I. Lei, R. Burnell, L. Bai, A. Gulati, G. Tanzer, D. Vincent, Z. Pan, S. Wang *et al.*, “Gemini 1.5: Unlocking multimodal understanding across millions of tokens of context,” *arXiv preprint arXiv:2403.05530*, 2024.
- [5] Z. Zhang, Y. Sheng, T. Zhou, T. Chen, L. Zheng, R. Cai, Z. Song, Y. Tian, C. Ré, C. Barrett *et al.*, “H2o: Heavy-hitter oracle for efficient generative inference of large language models,” *Advances in Neural Information Processing Systems*, vol. 36, pp. 34 661–34 710, 2023.
- [6] G. Xiao, Y. Tian, B. Chen, S. Han, and M. Lewis, “Efficient streaming language models with attention sinks,” *arXiv preprint arXiv:2309.17453*, 2023.
- [7] S. Ge, Y. Zhang, L. Liu, M. Zhang, J. Han, and J. Gao, “Model tells you what to discard: Adaptive kv cache compression for llms,” *arXiv preprint arXiv:2310.01801*, 2023.
- [8] Y. Li, Y. Huang, B. Yang, B. Venkitesh, A. Locatelli, H. Ye, T. Cai, P. Lewis, and D. Chen, “Snapkv: Llm knows what you are looking for before generation,” *arXiv preprint arXiv:2404.14469*, 2024.
- [9] Z. Liu, A. Desai, F. Liao, W. Wang, V. Xie, Z. Xu, A. Kyrillidis, and A. Shrivastava, “Scissorhands: Exploiting the persistence of importance hypothesis for llm kv cache compression at test time,” *Advances in Neural Information Processing Systems*, vol. 36, 2024.
- [10] C. Hooper, S. Kim, H. Mohammadzadeh, M. W. Mahoney, Y. S. Shao, K. Keutzer, and A. Gholami, “Kvquant: Towards 10 million context length llm inference with kv cache quantization,” *arXiv preprint arXiv:2401.18079*, 2024.
- [11] Z. Liu, J. Yuan, H. Jin, S. Zhong, Z. Xu, V. Braverman, B. Chen, and X. Hu, “Kivi: A tuning-free asymmetric 2bit quantization for kv cache,” *arXiv preprint arXiv:2402.02750*, 2024.
- [12] Y. Xu, Z. Jie, H. Dong, L. Wang, X. Lu, A. Zhou, A. Saha, C. Xiong, and D. Sahoo, “Think: Thinner key cache by query-driven pruning,” *arXiv preprint arXiv:2407.21018*, 2024.
- [13] Y. Zhang, Y. Du, G. Luo, Y. Zhong, Z. Zhang, S. Liu, and R. Ji, “Cam: Cache merging for memory-efficient llms inference,” in *Forty-first International Conference on Machine Learning*.
- [14] Z. Wang, B. Jin, Z. Yu, and M. Zhang, “Model tells you where to merge: Adaptive kv cache merging for llms on long-context tasks,” *arXiv preprint arXiv:2407.08454*, 2024.

- [15] Z. Wan, X. Wu, Y. Zhang, Y. Xin, C. Tao, Z. Zhu, X. Wang, S. Luo, J. Xiong, and M. Zhang, “D2o: Dynamic discriminative operations for efficient generative inference of large language models,” *arXiv preprint arXiv:2406.13035*, 2024.
- [16] D. Bolya, C.-Y. Fu, X. Dai, P. Zhang, C. Feichtenhofer, and J. Hoffman, “Token merging: Your vit but faster,” *arXiv preprint arXiv:2210.09461*, 2022.
- [17] A. Dosovitskiy, “An image is worth 16x16 words: Transformers for image recognition at scale,” *arXiv preprint arXiv:2010.11929*, 2020.
- [18] C. Hooper, S. Kim, H. Mohammadzadeh, M. Maheswaran, J. Paik, M. W. Mahoney, K. Keutzer, and A. Gholami, “Squeezed attention: Accelerating long context length llm inference,” *arXiv preprint arXiv:2411.09688*, 2024.
- [19] G. Liu, C. Li, J. Zhao, C. Zhang, and M. Guo, “Clusterkv: Manipulating llm kv cache in semantic space for recallable compression,” *arXiv preprint arXiv:2412.03213*, 2024.
- [20] D. Bolya and J. Hoffman, “Token merging for fast stable diffusion,” in *Proceedings of the IEEE/CVF conference on computer vision and pattern recognition*, 2023, pp. 4599–4603.
- [21] M. Kim, S. Gao, Y.-C. Hsu, Y. Shen, and H. Jin, “Token fusion: Bridging the gap between token pruning and token merging,” in *Proceedings of the IEEE/CVF Winter Conference on Applications of Computer Vision*, 2024, pp. 1383–1392.
- [22] H.-C. Tran, D. M. Nguyen, D. M. Nguyen, T.-T. Nguyen, N. Le, P. Xie, D. Sonntag, J. Y. Zou, B. T. Nguyen, and M. Niepert, “Accelerating transformers with spectrum-preserving token merging,” *arXiv preprint arXiv:2405.16148*, 2024.
- [23] R. Rombach, A. Blattmann, D. Lorenz, P. Esser, and B. Ommer, “High-resolution image synthesis with latent diffusion models,” in *Proceedings of the IEEE/CVF conference on computer vision and pattern recognition*, 2022, pp. 10 684–10 695.
- [24] Together, “Llama-2-7b-32k-instruct — and fine-tuning for llama-2 models with together api,” June 2023. [Online]. Available: <https://www.together.ai/blog/llama-2-7b-32k-instruct>
- [25] S. Merity, C. Xiong, J. Bradbury, and R. Socher, “Pointer sentinel mixture models,” *arXiv preprint arXiv:1609.07843*, 2016.
- [26] D. Yang, X. Han, Y. Gao, Y. Hu, S. Zhang, and H. Zhao, “Pyramidinfer: Pyramid kv cache compression for high-throughput llm inference,” *arXiv preprint arXiv:2405.12532*, 2024.
- [27] Z. Cai, Y. Zhang, B. Gao, Y. Liu, T. Liu, K. Lu, W. Xiong, Y. Dong, B. Chang, J. Hu *et al.*, “Pyramidkv: Dynamic kv cache compression based on pyramidal information funneling,” *arXiv preprint arXiv:2406.02069*, 2024.
- [28] H. Tang, Y. Lin, J. Lin, Q. Han, S. Hong, Y. Yao, and G. Wang, “Razorattention: Efficient kv cache compression through retrieval heads,” *arXiv preprint arXiv:2407.15891*, 2024.
- [29] Y. Feng, J. Lv, Y. Cao, X. Xie, and S. K. Zhou, “Ada-kv: Optimizing kv cache eviction by adaptive budget allocation for efficient llm inference,” *arXiv preprint arXiv:2407.11550*, 2024.
- [30] G. Xiao, J. Tang, J. Zuo, J. Guo, S. Yang, H. Tang, Y. Fu, and S. Han, “Duoattention: Efficient long-context llm inference with retrieval and streaming heads,” *arXiv preprint arXiv:2410.10819*, 2024.
- [31] Z. Shi, Y. Ming, X.-P. Nguyen, Y. Liang, and S. Joty, “Discovering the gems in early layers: Accelerating long-context llms with 1000x input token reduction,” *arXiv preprint arXiv:2409.17422*, 2024.
- [32] Y. Bai, X. Lv, J. Zhang, H. Lyu, J. Tang, Z. Huang, Z. Du, X. Liu, A. Zeng, L. Hou *et al.*, “Longbench: A bilingual, multitask benchmark for long context understanding,” *arXiv preprint arXiv:2308.14508*, 2023.
- [33] G. Kamradt, “Needle in a haystack: Evaluating long-context retrieval in language models,” Online, 2024, a benchmark for testing LLMs’ ability to retrieve specific information from long-context inputs. [Online]. Available: https://github.com/gkamradt/LLMTest_NeedleInAHaystack
- [34] A. Meta, “Introducing meta llama 3: The most capable openly available llm to date,” *Meta AI*, 2024.
- [35] J. Bai, S. Bai, Y. Chu, Z. Cui, K. Dang, X. Deng, Y. Fan, W. Ge, Y. Han, F. Huang *et al.*, “Qwen technical report,” *arXiv preprint arXiv:2309.16609*, 2023.

- [36] J. Tang, Y. Zhao, K. Zhu, G. Xiao, B. Kasikci, and S. Han, “Quest: Query-aware sparsity for efficient long-context llm inference,” *arXiv preprint arXiv:2406.10774*, 2024.
- [37] T. Wolf, “Huggingface’s transformers: State-of-the-art natural language processing,” *arXiv preprint arXiv:1910.03771*, 2019.

A Proof of Theorem 6.1

Proof. When $n = 1$, the result is trivial. In the following, we assume $n \geq 2$. Consider the following mapping:

$$\begin{aligned} \phi_{2n} : \mathbb{Z} &\rightarrow [2n] \\ x &\mapsto \begin{cases} 1, & x < 1; \\ x, & x \in [2n]; \\ 2n, & x > 2n; \end{cases} \end{aligned}$$

For any $l \in [2n - 1]$, define $\mathcal{S}_{2n,l} := \{(\phi_{2n}(x), \phi_{2n}(x + l)) \mid x \in \mathbb{Z} \cap [-l + 2, 2n - 1]\}$. For $\forall (A, B) \in \mathcal{P}_{2n}$, define

$$\mathcal{E}_{A,B} := \{(\min\{a, b\}, \max\{a, b\}) \mid a \in A \text{ and } b \in B\}, \quad (4)$$

$$\mathcal{D}_{A,B,l} := \{(a, b) \in \mathcal{E}_{A,B} \mid b - a = l\}, \quad (5)$$

$$\mathcal{T}_{A,B,l} := \{(a, b; c, d) \in [2n]^4 \mid (a, b) \in \mathcal{S}_{2n,l}, (c, d) \in \mathcal{E}_{A,B}, \text{ and } [c, d] \subseteq [a, b]\}, \quad (6)$$

Now we calculate the number of elements in $\mathcal{T}_{A,B,l}$, i.e., $|\mathcal{T}_{A,B,l}|$. Define $\mathcal{K}_{A,B,a,b} := \{(c, d) \in \mathcal{E}_{A,B} \mid [c, d] \subseteq [a, b]\}$, it holds that

$$|\mathcal{T}_{A,B,l}| = \sum_{(a,b) \in \mathcal{S}_{2n,l}} |\mathcal{K}_{A,B,a,b}|. \quad (7)$$

Note that

$$|\mathcal{K}_{A,B,a,b}| = |[a, b] \cap A| \cdot |[a, b] \cap B| \leq \left\lfloor \frac{b - a + 1}{2} \right\rfloor \cdot \left\lceil \frac{b - a + 1}{2} \right\rceil, \quad (8)$$

applying (8) to (7) yields

$$\begin{aligned} |\mathcal{T}_{A,B,l}| &\leq \sum_{(a,b) \in \mathcal{S}_{2n,l}} \left\lfloor \frac{b - a + 1}{2} \right\rfloor \cdot \left\lceil \frac{b - a + 1}{2} \right\rceil \\ &= \sum_{i=2}^l \left\lfloor \frac{i - 1 + 1}{2} \right\rfloor \cdot \left\lceil \frac{i - 1 + 1}{2} \right\rceil + \sum_{i=1}^{2n-l} \left\lfloor \frac{(i + l) - i + 1}{2} \right\rfloor \cdot \left\lceil \frac{(i + l) - i + 1}{2} \right\rceil + \\ &\quad + \sum_{i=2n-l+1}^{2n-1} \left\lfloor \frac{2n - i + 1}{2} \right\rfloor \cdot \left\lceil \frac{2n - i + 1}{2} \right\rceil \\ &= \begin{cases} -\frac{1}{12}l^3 + \frac{2n-1}{4}l^2 + \frac{6n-1}{6}l, & 2 \mid l; \\ -\frac{1}{12}l^3 + \frac{2n-1}{4}l^2 + \frac{12n-5}{12}l + \frac{2n-1}{4}, & 2 \nmid l. \end{cases} \triangleq c_{2n,l}. \end{aligned} \quad (9)$$

On the other hand, define $\mathcal{K}'_{2n,l,c,d} := \{(a, b) \in \mathcal{S}_{2n,l} \mid [c, d] \subseteq [a, b]\}$, we have

$$|\mathcal{K}'_{2n,l,c,d}| = \max(l + 1 - d + c, 0),$$

thus

$$\begin{aligned} |\mathcal{T}_{A,B,l}| &= \sum_{(c,d) \in \mathcal{E}_{A,B}} |\mathcal{K}'_{2n,l,c,d}| \\ &= \sum_{(c,d) \in \mathcal{E}_{A,B}} \max(l + 1 - d + c, 0) \\ &= \sum_{i=1}^l (l + 1 - i) |\mathcal{D}_{A,B,i}|. \end{aligned} \quad (10)$$

Combining (9)(10) yields

$$\sum_{i=1}^l (l + 1 - i) |\mathcal{D}_{A,B,i}| \leq c_{2n,l}. \quad (11)$$

Define $a_i = f(i) - f(i+1)$ for $i \in [2n-2]$, $b_i = a_i - a_{i+1}$ for $i \in [2n-3]$, and let $b_{2n-2} = a_{2n-2}$, it holds that $b_1, b_2, \dots, b_{2n-2} \geq 0$. Note that

$$\begin{aligned} f(i) &= f(2n-1) + \sum_{j=i}^{2n-2} a_j, \\ &= f(2n-1) + \sum_{j=i}^{2n-2} \sum_{k=j}^{2n-2} b_k, \\ &= f(2n-1) + \sum_{j=i}^{2n-2} (j-i+1)b_j, \quad \forall i \in [2n-2], \end{aligned}$$

we have

$$\begin{aligned} \sum_{x \in A} \sum_{y \in B} f(|x-y|) &= \sum_{i=1}^{2n-1} |\mathcal{D}_{A,B,i}| f(i) \\ &= \sum_{i=1}^{2n-1} |\mathcal{D}_{A,B,i}| \left(f(2n-1) + \sum_{j=i}^{2n-2} (j-i+1)b_j \right) \\ &= |\mathcal{E}_{A,B}| f(2n-1) + \sum_{j=1}^{2n-2} \sum_{i=1}^j (j+1-i) |\mathcal{D}_{A,B,i}| b_j \\ &\leq n^2 f(2n-1) + \sum_{j=1}^{2n-2} c_{2n,j} b_j, \end{aligned} \tag{12}$$

where the last inequality uses $|\mathcal{E}_{A,B}| = n^2$ and (11). If $A_0 = \{1, 3, \dots, 2n-1\}$ and $B_0 = \{2, 4, \dots, 2n\}$, we have

$$\begin{aligned} \sum_{x \in A_0} \sum_{y \in B_0} f(|x-y|) &= \sum_{i=1}^{2n-1} |\mathcal{D}_{A_0,B_0,i}| f(i) = \sum_{i=1}^n |\mathcal{D}_{A_0,B_0,2i-1}| f(2i-1) \\ &= \sum_{i=1}^n (2n-2i+1) \left(f(2n-1) + \sum_{j=2i-1}^{2n-2} (j-2i+2)b_j \right) \\ &= n^2 f(2n-1) + \sum_{j=1}^{2n-2} \sum_{i=1}^{\lfloor \frac{j+1}{2} \rfloor} (2n-2i+1)(j-2i+2)b_j. \end{aligned} \tag{13}$$

Note that

$$\sum_{i=1}^{\lfloor \frac{j+1}{2} \rfloor} (2n-2i+1)(j-2i+2) = \begin{cases} -\frac{1}{12}l^3 + \frac{2n-1}{4}l^2 + \frac{6n-1}{6}l, & 2 \mid l; \\ -\frac{1}{12}l^3 + \frac{2n-1}{4}l^2 + \frac{12n-5}{12}l + \frac{2n-1}{4}, & 2 \nmid l. \end{cases} = c_{2n,j}, \tag{14}$$

combining (13)(14) yields

$$\sum_{x \in A_0} \sum_{y \in B_0} f(|x-y|) = n^2 f(2n-1) + \sum_{j=1}^{2n-2} c_{2n,j} b_j. \tag{15}$$

Combining (12)(15), we obtain

$$(A_0, B_0) \in \arg \max_{(A,B) \in \mathcal{P}_{2n}} \sum_{x \in A} \sum_{y \in B} f(|x-y|),$$

which concludes the proof. \square

B Outlier head identification

We use the widely adopted WikiText-2 [25] dataset for calibration. As shown in Fig. 1, each token in set A is connected to its most similar token in set B by an edge in Chunked Soft Matching algorithm. To identify outlier heads, we set the edge similarity threshold to 0.8, prune edges with lower similarity, and calculate the proportion of tokens in set A without any connected edges after pruning. We randomly sample sequences and average the proportion values for each head. Offline calibration visualizations are presented in Fig. 6 and Fig. 7 for Llama-2 and Llama-3, respectively. Outlier heads only have a small proportion of tokens that are connected by edges with a similarity greater than 0.8, indicating that these heads are more sensitive to similarity-based clustering. Notably, the number of outlier heads is minimal, thereby does not significantly affect the overall performance of our approach.

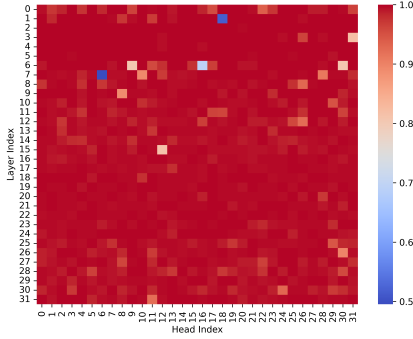


Figure 6: Outlier heads of Llama2-7b-32K.

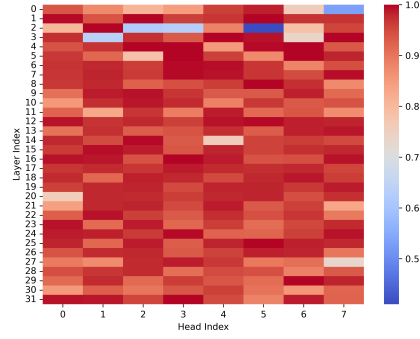


Figure 7: Outlier heads of Llama3.1-8b-Instruct.

C Experimental Details

C.1 Baseline settings

For SnapKV [8], we use the last 100 tokens as the observation window to accumulate historical information. For StreamingLLM [6], as recommended in the paper, we take the first 4 tokens as the attention sinks. CaM [13] rely on a preliminary token eviction method to identify the merging set. To support long context inference, we employ StreamingLLM as its pre-merging eviction strategy, which is consistent with the original paper.

C.2 Chelsea settings

We set the outlier head ratio for each model as 4%. For layer-wise similarity differences, we retain the first layer of Llama-2, which is included in the outlier head ratio. We apply the same compression process to all layers in Llama-3, as our experiments show that the benefits are marginal. To ensure a fair comparison, we reallocate the budget between layers and heads to keep the total budget consistent across all methods.

The discussion about the compression ratio r is as follows. Since the Chunked Soft Matching mechanism can reduce the cache size by at most half at each step, r is constrained within the range $0 \leq r \leq 0.5$. Intuitively, the similarity score between tokens tends to decrease as the number of clustering steps increases. Empirically, we have found that using a decreasing compression ratio r in the initial steps enhances model performance, which means r follows the rule:

$$r = r_{\text{init}} - \alpha \cdot \min(m, i)$$

where r_{init} is the initial ratio, α represents the decrease rate, m is number of initial steps, and i is the current clustering step starting from 0. Based on the calibration similarity map, we set $r_{\text{init}} = 0.45, m = 3, \alpha = 0.05$ for Llama-2, $r_{\text{init}} = 0.35, m = 2, \alpha = 0.1$ for Llama-3 and $r_{\text{init}} = 0.2, m = 2, \alpha = 0.1$ for Qwen, where r is manually restricted to exceed 0.

Table 6: Complete results of LongBench on Llama-2-7b-32K with 20% KV cache budget.

Dataset	StreamingLLM	SnapKV	CaM	Chelsea	Full
NarrativeQA	16.72	21.78	18.04	22.74	20.53
Qsper	18.67	24.63	18.78	31.2	34.95
MultiFieldQA-en	18.63	25.52	18.96	30.38	34.77
MultiFieldQA-zh	12.43	25.34	12.34	24.08	32.85
HotpotQA	41.6	45.72	41.25	46.51	49.11
2WikiMQA	29.67	35.87	29.16	36.49	36.61
Musique	16.69	20.45	16.91	20.49	21.87
DuReader (zh)	13.24	12.14	13.17	16.07	19.02
GovReport	17.3	13.13	17.06	16.28	29.01
QMSum	15.85	17.51	15.83	16.67	17.15
MultiNews	4.33	2.6	4.4	16.23	21.62
VCSUM (zh)	8.58	5.51	8.66	7.85	9.39
TREC	55.0	50.0	55.0	71.0	71.5
TriviaQA	84.66	85.46	84.66	87.37	87.79
SAMSum	37.95	40.04	38.78	40.86	43.89
LSHT(zh)	23.5	19.5	23.0	18.0	31.5
Passage Count	2.0	2.0	2.0	2.0	1.5
PassageRetrieval-en	16.5	18.0	16.5	23.0	21.0
PassageRetrieval-zh	4.52	4.54	5.52	5.88	6.82
LCC	29.98	25.58	29.84	47.37	50.84
RepoBench-P	47.86	46.87	47.87	48.93	50.66

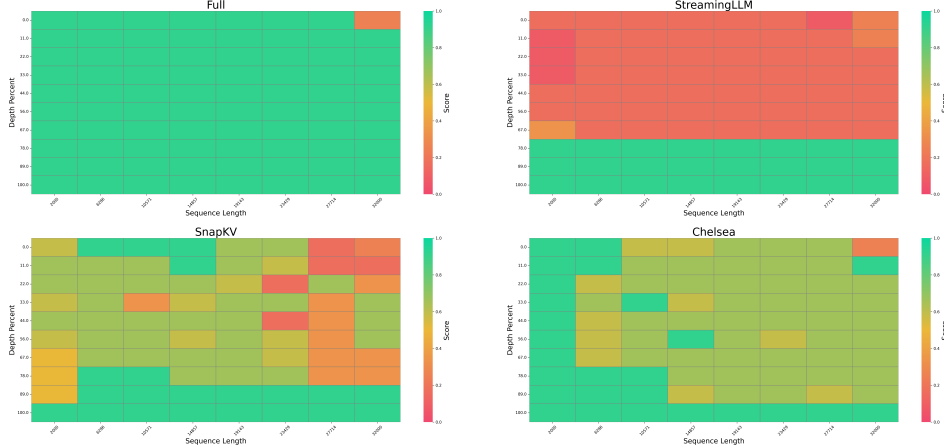


Figure 8: Llama-2-7b-32K on Needle-in-a-Haystack benchmark, under 25% KV cache budget.

D Additional Results

D.1 Accuracy evaluation

In addition to the performance comparison presented in Fig. 4 and Table 2, we further provide the complete results for LongBench datasets with 20% KV cache budget in Table 6, Table 7 and Table 8.

In addition to LongBench, we also conducted experiments on a widely used benchmark Needle in a Haystack. Fig. 8 further demonstrate that Chelsea outperforms existing methods across multiple tasks. Notably, the impact of outlier head is small in this task, we omit it and apply a constant compression ratio 0.25.

D.2 Efficiency evaluation

In addition to Table 3, we present the inference latency and GPU memory usage comparison on Llama-2-7b-32K in Table 9. When the context length is 64K, full attention and CaM result in a CUDA

Table 7: Complete results of LongBench on Llama-3.1-8b-instruct with 20% KV cache budget.

Dataset	StreamingLLM	SnapKV	CaM	Chelsea	Full
NarrativeQA	26.62	31.51	27.05	31.61	31.69
Qsper	13.49	18.21	13.76	20.37	26.25
MultiFieldQA-en	16.74	22.45	16.31	26.32	28.71
MultiFieldQA-zh	11.21	16.62	11.22	17.01	20.08
HotpotQA	12.36	15.42	12.62	16.52	17.01
2WikiMQA	13.14	14.64	12.88	15.61	16.3
Musique	7.88	11.88	7.78	11.42	11.59
DuReader (zh)	14.03	19.55	14.06	24.08	29.67
GovReport	28.05	27.43	27.96	26.32	34.73
QMSum	20.9	22.67	20.97	22.31	23.5
MultiNews	22.31	23.02	22.29	24.33	26.91
VCSUM (zh)	14.41	14.71	14.44	14.73	16.33
TREC	65.0	64.0	65.0	73.5	72.5
TriviaQA	89.74	90.53	89.79	91.25	91.65
SAMSum	42.36	42.27	41.83	41.45	43.94
LSHT(zh)	32.5	40.5	32.5	43.0	46.5
Passage Count	7.01	6.5	7.61	6.28	5.35
PassageRetrieval-en	93.58	97.46	93.54	97.98	98.23
PassageRetrieval-zh	26.19	75.12	26.19	87.09	78.07
LCC	50.41	51.84	50.24	49.52	52.16
RepoBench-P	47.15	49.2	47.12	48.21	48.79

Table 8: Complete results of LongBench on Qwen2-7B-Instruct with 20% KV cache budget.

Dataset	StreamingLLM	SnapKV	CaM	Chelsea	Full
NarrativeQA	22.82	25.92	22.63	24.8	25.42
Qasper	31.67	37.91	31.91	43.6	45.92
MultiFieldQA-en	27.46	44.23	27.17	44.27	48.22
MultiFieldQA-zh	35.44	53.76	35.05	57.65	59.78
HotpotQA	34.25	41.15	34.33	41.39	42.89
2WikiMQA	37.23	43.97	37.69	42.81	44.99
Musique	17.69	24.32	17.65	24.84	24.8
DuReader (zh)	16.35	21.34	16.34	22.2	26.38
GovReport	25.42	26.33	25.35	12.65	34.36
QMSum	20.52	22.29	20.39	21.2	23.67
MultiNews	20.74	21.98	21.05	22.57	26.13
VCSUM (zh)	15.68	15.66	15.82	12.86	17.45
TREC	45.0	40.0	45.0	51.0	52.5
TriviaQA	83.43	83.74	83.5	84.56	84.09
SAMSum	34.05	34.59	33.91	33.39	35.64
LSHT(zh)	13.43	32.25	13.89	36.89	38.98
Passage Count	5.0	5.5	5.0	5.0	5.5
PassageRetrieval-en	29.5	65.5	28.5	71.5	70.5
PassageRetrieval-zh	22.0	49.0	21.5	53.0	55.0
LCC	44.17	44.77	43.84	47.25	47.16
RepoBench-P	41.85	43.4	41.82	41.91	44.09

out-of-memory error. In contrast, Chelsea keep its performance with highly efficient framework and can support extremely long context inference.

D.3 Ablation study

Importance of chunking. The detailed inference latency comparison between Chelsea and its variant without chunking is presented in Table 10. The results show that chunking significantly accelerates the clustering process by avoiding the computation of prohibitively large similarity matrices. Designed

Table 9: Decoding latency and GPU memory usage (GB) comparison across varying context lengths on Llama-2-7b-32K. Time To First Token (s) and Time Per Output Token (s) are based on HuggingFace Transformers. OOM refers to a CUDA out-of-memory error.

Context Length	16k			32k			64k		
	TTFT	TPOT	Memory	TTFT	TPOT	Memory	TTFT	TPOT	Memory
Full	1.659	0.047	29.16	3.959	0.079	44.79		OOM	
CaM	1.680	0.070	29.20	3.987	0.106	44.86		OOM	
Chelsea	1.798	0.032 (1.47 \times)	15.91	4.275	0.032 (2.47 \times)	19.04	11.408	0.047	25.31

Table 10: Time To First Token (s) and Time Per Output Token (s) based on HuggingFace Transformers. OOM refers to CUDA out-of-memory error. The clustering overhead is largely reduced by chunking.

Context Length		16k		32k		64k	
Model	Chunking	TTFT	TPOT	TTFT	TPOT	TTFT	TPOT
Llama-2-7B	\times	2.097	0.032	5.456	0.034	OOM	
	\checkmark	1.798	0.032	4.275	0.035	11.408	0.047
Llama-3.1-8B	\times	1.842	0.035	4.526	0.036	13.156	0.044
	\checkmark	1.814	0.035	4.306	0.036	11.500	0.043

with simplicity and efficiency in mind, Chelsea minimizes additional computational overhead while achieving substantial speedup.

Table 11: The identification of outlier heads further improves Chelsea’s performance.

Dataset	StreamingLLM	SnapKV	Chelsea (w/o outlier head)	Chelsea
Qsper	18.67	24.63	28.35	31.2
MultiFieldQA-en	18.63	25.52	27.52	30.38
2WikiMQA	29.67	35.87	34.7	36.49
DuReader (zh)	13.24	12.14	15.33	16.07
MultiNews	4.33	2.6	11.34	16.23
TREC	55.0	50.0	68.0	71.0
TriviaQA	84.66	85.46	86.21	87.37
PassageRetrieval-en	16.5	18.0	20.25	23.0
Average	30.10	31.78	36.46	38.97

Importance of outlier heads. To further highlight the significance of outlier heads, we select a range of tasks from LongBench and present a detailed accuracy comparison with a 20% KV cache budget in Table 11. The identification of outlier heads and the subsequent reallocation of the KV cache budget lead to additional improvements in Chelsea’s performance. Notably, even without the consideration of outlier heads, Chelsea consistently outperforms the baseline methods, further underscoring the superiority of clustering-based compression over eviction-based methods.